DOI: 10.1002/ejic.201000753

A Novel Water-Soluble Hexanuclear Bismuth Oxido Cluster – Synthesis, Structure and Complexation with Polyacrylate

Linda Miersch,[a] Tobias Rüffer,[b] Heinrich Lang,[b] Steffen Schulze,[c] Michael Hietschold,[c] Dirk Zahn,*[d] and Michael Mehring*[a]

Keywords: Bismuth / Cluster compounds / Polymers / Molecular dynamics / Organic–inorganic hybrid materials

The reaction of $[Bi_6O_4(OH)_4](NO_3)_6{\cdot}H_2O$ with triflic acid gave colorless single crystals of $[Bi_6O_4(OH)_4(OTf)_6(CH_3CN)_6]{\cdot}2CH_3CN$ (**1**) upon crystallization from acetonitrile/chloroform. Compound **1** crystallizes in the monoclinic space group $P2_1/n$. The novel hexanuclear bismuth oxido cluster is highly soluble in water and polar organic solvents. A transparent and water-soluble hybrid material was obtained by reaction of $[Bi_6O_4(OH)_4(OTf)_6(CH_3CN)_6]{\cdot}2CH_3CN$ (**1**) with polyacrylate in aqueous solution. Molecular dynamics simulations were performed to study the complexation behavior of the $[Bi_6O_{4+x}(OH)_{4-x}]^{(6-x)+}$ cation with polyacrylate in solution.

Introduction

Most bismuth-containing compounds are considered to be nontoxic, which is mainly attributed to their low solubility in neutral aqueous solution. This involves only a poor absorption of bismuth from the alimentary tract, skin, and musculature.[1,2] However, in some cases a bismuth-induced encephalopathy as a consequence of an ingestion of bismuth-containing remedies was reported, possibly as a result of biomethylation in the human body.[2,3] Nevertheless bismuth(III) salts such as neutral and basic bismuth nitrates as well as bismuth potassium tartrate, basic carbonate, and bismuth subsalicylate are widely used in therapy without showing adverse side effects.[4] So called bismuth subsalicylate and subcitrate have found medical application as active ingredients of pharmaceuticals, for example Pepto-Bismol® and DE-NOL™, for the treatment of indigestion, upset stomach, and diarrhea.[5] Furthermore, it was reported that bismuth(III) complexes could significantly reduce toxic side effects of the anticancer drug cisplatin without compromising its antitumor activity.[6] In cosmetics, BiOCl is used to give a pearlescent effect. In addition to their almost non-toxic behavior, bismuth-containing materials show high radiopacity, and thus some of them are investigated as potential X-ray imaging agents for computed tomography (CT) and as X-ray contrast additives in bone and dental cements, for example, to enable postoperative examination of their anchorage, texture, and form fit.[7,8] Conventional radio contrast media like barium sulfate or zirconium dioxide can cause a greater osteolytically induced loss than bismuth-containing cements.[8,9] Furthermore, the addition of barium sulfate causes an incompatibility between the metal salt and the polymer, hence the mechanical strength and fracture toughness of the bone cement is affected.[8] Other radiopaque bismuth-containing fillers such as $Bi(NO_3)_3$, $BiBr_3$, $Bi_2O_2(CO_3)$, and Bi_2O_3 were suggested, and their use was patented.[10,11] A major disadvantage associated with the low solubility of these inorganic bismuth compounds is phase separation due to their incompatibility with the organic matrix. In addition to the danger of leaching, adverse effects on the mechanical or esthetic properties of the resulting materials may be induced.[11] $BiPh_3$ was mentioned in the literature as another promising X-ray contrast additive in PMMA-based bone cements.[8,9,11] This organobismuth compound is hydrophobic and possesses antimicrobial, fungicidal, and antioxidant properties, but its application in dental and bone cements holds the danger of the formation of toxic thermal and photochemical decomposition products.[8]

We have been interested in bismuth oxido clusters as molecular precursors to materials based on bismuth oxide for several years now.[12,13] In addition to our reports on different bismuth oxido clusters with up to 22 bismuth atoms formed by partial hydrolysis of bismuth(III) silanolates, other large bismuth oxido clusters with up to 38 bismuth atoms have been reported by the groups of Andrews and

[a] Professur für Koordinationschemie, Technische Universität Chemnitz,
Straße der Nationen 62, 09111 Chemnitz, Germany
Fax: +49-371-531-21219
E-mail: michael.mehring@chemie.tu-chemnitz.de
[b] Professur für Anorganische Chemie, Technische Universität Chemnitz,
Straße der Nationen 62, 09111 Chemnitz, Germany
[c] Professur für Analytik an Festkörperoberflächen, Technische Universität Chemnitz,
Reichenhainer Str. 70, 09126 Chemnitz, Germany
[d] Professur für Theoretische Chemie, Friedrich-Alexander-Universität Erlangen-Nürnberg,
Nägelsbachstr. 25, 91052 Erlangen, Germany

Dikarev.[12,14] Additional examples of bismuth oxido clusters include the triflate $[Bi_9O_8(OH)_6(CF_3SO_3)_5]$,[15] the phosphonate $[(tBuPO_3)_{10}(tBuPO_3H)_2Bi_{14}O_{10}\cdot 3C_6H_6\cdot 4H_2O]$,[16] and the aryl oxide $[Bi_{32}O_{40}(OH)_4(O\text{-}2,6\text{-}Ph_2C_6H_3)_{12}]$.[17] The majority of these compounds have low solubility, are sensitive towards water, or are accessible only with low yield. Thus they do not hold potential for the synthesis of homogeneous hybrid materials. Currently, we are focusing on the synthesis of highly soluble bismuth oxido clusters, which can be embedded into a matrix consisting of polymers such as polyacrylate to obtain a good dispersity of bismuth in a hybrid material. It is noteworthy that in several patents the use of pharmaceuticals containing water-based dispersions of compounds of bismuth and polyacrylic acid has already been proposed for the treatment of inflammatory bowel disease.[18] Herein we report the preparation of a water-soluble hybrid material starting from the novel hexanuclear bismuth oxido cluster $[Bi_6O_4(OH)_4(OTf)_6(CH_3CN)_6]\cdot 2CH_3CN$ (**1**) and polyacrylate.

Results and Discussion

The formation of the hexanuclear cation $[Bi_6O_4(OH)_4]^{6+}$ upon hydrolysis of bismuth(III) nitrate in acidic solution was demonstrated by single-crystal X-ray diffraction analysis by Lazarini and Sundvall for the first time.[19,20] The $[Bi_6O_4(OH)_4]^{6+}$ cation is formed by hydrolysis of hydrated Bi^{3+} in concentrated (0.1 M) aqueous solution of the bismuth(III) salt at a pH value of 0–3.[21] Compounds consisting of the $[Bi_6O_4(OH)_4]^{6+}$ fragment as central structural unit, such as $[Bi_6O_4(OH)_4](NO_3)_6\cdot(H_2O)_n$, $[Bi_6O_4(OH)_4](ClO_4)_6\cdot(H_2O)_7$, $[Bi_6O_4(OH)_4(tfa)_6][Bi(tfa)_3]_3$ (tfa = $CF_3CO_2^-$), and $[Bi_6O_4(OH)_4(NTf_2)_6(H_2O)_6]$ {NTf_2 = $N(O_2SCF_3)_2^-$}, were obtained by hydrolysis of the respective bismuth(III) salt.[19,22,23] The title compound, $[Bi_6O_4(OH)_4(OTf)_6(CH_3CN)_6]\cdot 2CH_3CN$ (**1**), represents an example of a highly soluble hexanuclear bismuth oxido cluster, which was prepared by reaction of $[Bi_6O_4(OH)_4](NO_3)_6\cdot H_2O$ with CF_3SO_3H in toluene. The complete exchange of nitrate by triflate is confirmed by IR spectroscopy and elemental analysis. The hexanuclear bismuth oxido core, $[Bi_6O_4(OH)_4]^{6+}$, is preserved during the reaction. Crystallization from acetonitrile/chloroform gave colorless single crystals of **1** suitable for single-crystal X-ray diffraction analysis. $[Bi_6O_4(OH)_4](NO_3)_6\cdot H_2O$ was synthesized as described previously by hydrolysis of $Bi(NO_3)_3\cdot 5H_2O$ in aqueous solution under acidic conditions to give the tetrahydrate followed by careful dehydration at 80 °C for 12 h.[19,24] In addition to the reaction of $[Bi_6O_4(OH)_4](NO_3)_6\cdot H_2O$ with CF_3SO_3H, it is possible to prepare compound **1** by reaction of $[Bi_6O_4(OH)_4](NO_3)_6\cdot H_2O$ with $Me_3SiO_3SCF_3$ in toluene.

$[Bi_6O_4(OH)_4(OTf)_6(CH_3CN)_6]\cdot 2CH_3CN$ (**1**) crystallizes in the monoclinic space group $P2_1/n$ with the lattice constants a = 12.6443(8) Å, b = 18.1326(4) Å, c = 27.0115(9) Å and β = 96.787(4)°; there are four formula units per unit cell.

Figure 1 shows the molecular structure of compound **1**, which is based on an octahedron with six bismuth atoms at its corners. The bismuth atoms are associated with eight μ_3-oxygen atoms with Bi–O bond lengths in the range of 2.11 to 2.87 Å (Figure 2, Table 1). Each of the μ_3-oxygen atoms is situated above an octahedral face. Four of the eight oxygen atoms belong to hydroxides. The positions of the hydrogen atoms could be located by single-crystal X-ray diffraction analysis. The IR spectrum shows a band centered at 3467 cm^{-1}, which is assigned to the hydroxy groups. In addition, the ^1H NMR spectrum shows a signal indicative of hydroxy protons, which is found in the range from 3.0 to 3.8 depending on the concentration.

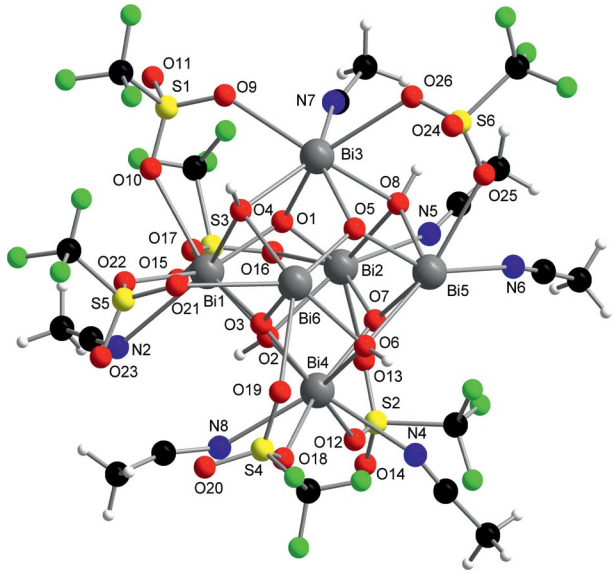

Figure 1. Ball-and-stick model of the molecular structure of $[Bi_6O_4(OH)_4(OTf)_6(CH_3CN)_6]\cdot 2CH_3CN$ (**1**). CH_3CN as packing solvent has been omitted.

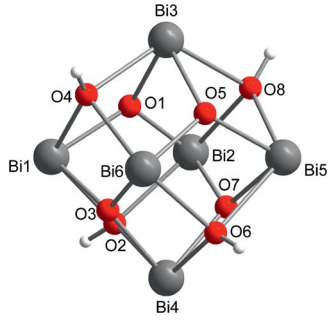

Figure 2. Ball-and-stick model of the hexanuclear bismuth oxido core of compound **1**.

Selected bond lengths and angles within the bismuth oxido core $[Bi_6O_4(OH)_4]^{6+}$ are listed in Table 1. While the average Bi–μ_3-OH distance is 2.40(4) Å, the Bi–μ_3-O bonds are shorter, with a mean value of 2.16(4) Å, which is as expected and consistent with a report on the molecular structure of $[Bi_6O_4(OH)_4](ClO_4)_6\cdot(H_2O)_7$.[22]

Table 1. Bi–O bond lengths and angles of the bismuth oxido core $[Bi_6O_4(OH)_4]^{6+}$ in $[Bi_6O_4(OH)_4(OTf)_6(CH_3CN)_6]\cdot 2CH_3CN$ (**1**).

$[Bi_6O_4(OH)_4]^{6+}$ unit in compound **1**			
Bi–μ_3-O		Bi–μ_3-OH	
Bond lengths [Å]			
Bi1–O1	2.139(11)	Bi1–O2	2.413(12)
Bi1–O3	2.187(11)	Bi1–O4	2.423(10)
Bi2–O7	2.134(12)	Bi2–O2	2.370(11)
Bi2–O1	2.147(12)	Bi2–O8	2.424(10)
Bi3–O1	2.156(12)	Bi3–O4	2.380(11)
Bi3–O5	2.191(11)	Bi3–O8	2.468(12)
Bi4–O7	2.178(12)	Bi4–O6	2.389(11)
Bi4–O3	2.189(11)	Bi4–O2	2.393(11)
Bi5–O5	2.173(11)	Bi5–O8	2.280(11)
Bi5–O7	2.184(11)	Bi5–O6	2.537(13)
Bi6–O3	2.114(11)	Bi6–O6	2.280(13)
Bi6–O5	2.150(11)	Bi6–O4	2.409(11)
Angles [°]			
O1–Bi1–O3	89.6(4)	O1–Bi3–O8	70.9(4)
O1–Bi1–O2	72.2(4)	O5–Bi3–O8	70.3(4)
O3–Bi1–O2	71.8(4)	O4–Bi3–O8	124.3(3)
O1–Bi1–O4	70.2(4)	O5–Bi5–O7	92.0(4)
O3–Bi1–O4	69.2(4)	O5–Bi5–O8	74.3(4)
O2–Bi1–O4	124.9(4)	O7–Bi5–O8	73.5(4)
O1–Bi3–O5	89.8(4)	O5–Bi5–O6	67.9(4)
O1–Bi3–O4	70.8(4)	O7–Bi5–O6	69.4(4)
O5–Bi3–O4	70.7(4)	O8–Bi5–O6	124.9(4)

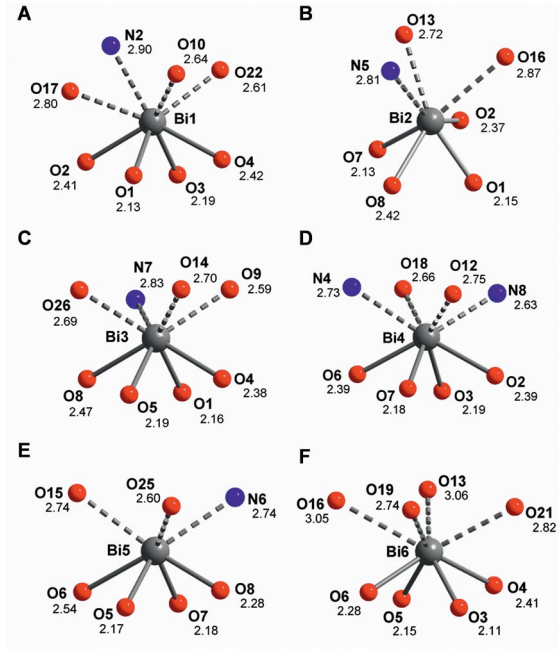

Figure 3. Bismuth coordination spheres in the bismuth oxido cluster $[Bi_6O_4(OH)_4(OTf)_6(CH_3CN)_6]\cdot 2CH_3CN$ (**1**). **A**, **C**, **D**, and **F** show [4+4] coordination. For **B** and **E** strongly distorted coordination polyhedra with [4+3] coordination are observed. The bond lengths are given in Å.

The Bi–Bi distances range from 3.6 to 3.8 Å, which is in fair agreement with the mean Bi–Bi distance of 3.7 Å in $[Bi_6O_4(OH)_4](NO_3)_6$ and other hexanuclear bismuth oxido compounds.[19,20,22,23,25] Bismuth atoms Bi1, Bi3, Bi4, and Bi6 show eightfold coordination, while Bi2 and Bi5 are sevenfold coordinated. The increase of the bismuth coordination up to eightfold is caused by additional coordination of one (Bi1–Bi3, Bi5) and two (Bi4) nitrogen atoms from the coordinated acetonitrile. The bismuth coordination geometries are strongly distorted. Such distortions are typical for bismuth oxido compounds and may be ascribed to the stereochemical activity of the lone pair at the bismuth atoms.[26,27] The coordination polyhedra can be described as square-based pseudopyramids with [4+3] (Bi2) and [4+4] (Bi1, Bi3–Bi6) coordination. The pyramids are capped by oxygen and nitrogen atoms (Figure 3). The bonding situation of the bismuth coordination spheres is best described by a bond pattern [X+Y] composed of short primary [X] and significantly longer secondary bonds [Y].[26] Here we propose that the primary bonds exhibit Bi–O distances in the range from 2.11 to 2.54 Å and the secondary bonds range from 2.55 to 3.06 Å, including Bi–N distances of 2.63–2.90 Å (Table 2).

The cationic $[Bi_6O_4(OH)_4]^{6+}$ unit is coordinated by six triflate groups in a bridging mode. One triflate anion coordinates via two oxygen atoms to two bismuth atoms of the central Bi_6O_8 core. With a mean length of 2.71 Å, these secondary Bi–O bonds are longer than the corresponding bonds within the bismuth oxido unit. An intermolecular connection of the proximate metal oxido unit with Bi3 and Bi5 is established via triflates O14–S2–O12/O13 and O15–S3–O16/O17, respectively, and this implicates the formation of a 1D polymeric chain along the crystallographic *b* axis (Figure 4). These chains extend across the crystal by forming layers, with CF_3 groups between them (Figure 5). The coordination of the triflate group to Bi3 and Bi5 causes an inclination of the $[Bi_6O_4(OH)_4]^{6+}$ units with respect to each other.

In contrast to most of the other bismuth oxido clusters reported so far, compound **1** is highly soluble in water (pH = 7 before and pH = 3 after dissolution of **1**) and polar organic solvents and thus is a suitable candidate for the synthesis of organic–inorganic hybrid materials in homogeneous solution, for example, starting from **1** and polyacrylate. The polyacrylate used for the synthesis of the organic–inorganic hybrid materials reported here was Sokalan® PA15. The Sokalan PA types are effective dispersing agents and have been found to perform well in phosphate-free laundry detergents. Their addition prevents graying and deposits of insoluble salts on fabrics and thus boosts detergency. Sokalan® PA15 contains an aqueous solution of approximately 45% sodium polyacrylate. The mean molecular weight of the polymer chains is 1200 g/mol. In addition to Sokalan® PA15, the polymer Sokalan® PA70 PN, with a mean molecular weight of 70000 g/mol, was tested for complexation.[28] However, the reaction of Sokalan® PA70 PN with compound **1** afforded insoluble materials, and we therefore focused on the reaction of the polyacrylate Sokalan® PA15 with $[Bi_6O_4(OH)_4(OTf)_6(CH_3CN)_6]\cdot 2CH_3CN$ (**1**).

Table 2. Selected bond lengths and angles of $[Bi_6O_4(OH)_4(OTf)_6(CH_3CN)_6]\cdot 2CH_3CN$ (**1**) with regard to secondary bonds.[a]

$[Bi_6O_4(OH)_4(OTf)_6(CH_3CN)_6]\cdot 2CH_3CN$ (**1**)			
Bond lengths [Å]			
Bi1–O10	2.642(13)	Bi2–N5	2.8121(1)
Bi1–O22	2.614(13)	Bi3–N7	2.8299(1)
Bi2–O13	2.723(12)	Bi4–N4B	2.7328(2)
Bi2–O16	2.867(12)	Bi4–N8	2.6340(1)
Bi3–O9	2.585(15)	Bi5–N6	2.7429(1)
Bi3–O14A	2.695(11)	S2–O12	1.432(12)
Bi3–O26A	2.694(13)	S2–O13	1.464(13)
Bi4–O12	2.748(11)	S2–O14	1.438(12)
Bi4–O18	2.664(17)	S3–O15	1.427(14)
Bi5–O15	2.743(13)	S3–O16	1.415(16)
Bi5–O25A	2.604(12)	S3–O17	1.462(14)
Bi6–O21	2.824(15)	S4–O18	1.419(17)
Bi6–O19	2.735(14)	S4–O19	1.449(15)
Bi1–N2	2.9018(1)	S4–O20	1.409(17)
Angles [°]			
O1–Bi1–O22	145.5(5)	O4–Bi3–O26A	134.6(4)
O3–Bi1–O22	86.2(4)	O8–Bi3–O26A	76.3(4)
O2–Bi1–O22	137.3(5)	O9–Bi3–O26A	118.2(4)
O4–Bi1–O22	76.4(4)	O14A–Bi3–O26A	70.4(4)
O1–Bi1–O10	85.4(4)	O7–Bi4–N8	143.0(6)
O3–Bi1–O10	143.0(4)	O3–Bi4–N8	84.8(8)
O2–Bi1–O10	139.5(4)	O6–Bi4–N8	137.7(8)
O4–Bi1–O10	74.6(4)	O2–Bi4–N8	72.6(6)
O22–Bi1–O10	77.8(5)	O5–Bi5–N6	146.4(5)
O7–Bi2–O13	87.5(4)	O7–Bi5–N6	87.8(5)
O1–Bi2–O13	149.7(4)	O8–Bi5–N6	73.4(5)
O2–Bi2–O13	78.0(4)	O6–Bi5–N6	141.3(5)
O8–Bi2–O13	135.5(4)	O25A–Bi5–N6	78.9(5)
O1–Bi3–O9	84.9(5)	O15–Bi5–N6	111.3(5)
O5–Bi3–O9	146.3(5)	O10–S1–O11	115.6(10)
O4–Bi3–O9	76.2(4)	O10–S1–O9	114.0(8)
O8–Bi3–O9	137.2(5)	O12–S2–O13	114.4(7)
O1–Bi3–O14A	141.6(4)	O14–S2–O13	114.7(7)
O5–Bi3–O14A	87.3(4)	O16–S3–O15	114.2(8)
O4–Bi3–O14A	72.2(4)	O16–S3–O17	114.6(9)
O8–Bi3–O14A	141.8(4)	O15–S3–O17	115.1(9)
O9–Bi3–O14A	76.9(4)	O18–S4–O19	112.5(10)
O1–Bi3–O26A	146.9(4)	O22–S5–O21	113.8(8)
O5–Bi3–O26A	82.7(4)	O25–S6–O26	113.0(7)

[a] Symmetry transformations used to generate equivalent atoms. A: $-x + 1/2$, $y - 1/2$, $-z + 1/2$; B: $x + 1$, y, z.

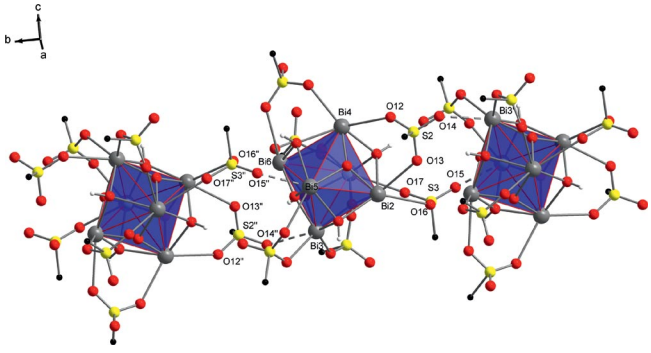

Figure 4. Selected part of a 1D chain in the solid state displaying the connectivity pattern of the molecular $[Bi_6O_4(OH)_4]^{6+}$ units bridged by triflate anions. F atoms of the CF_3 groups and CH_3CN are omitted for clarity.

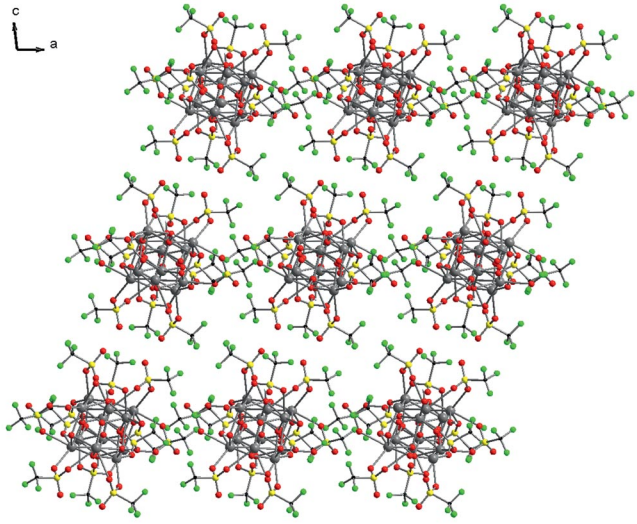

Figure 5. View of the 1D chains along the crystallographic *b* axis. CH_3CN has been omitted for clarity.

In a typical procedure, the organic–inorganic hybrid materials were prepared by mixing aqueous solutions of Sokalan® PA15 and **1**. Subsequent addition of acetone causes a phase separation to occur, and a viscous gel is obtained. Vacuum drying of the separated gel gives a water-soluble transparent solid. The synthesis was performed with a starting bismuth content of 10% at a pH value of 2.84. At a pH range between 0 and 3, the cationic $[Bi_6O_{4+x}(OH)_{4-x}]^{(6-x)+}$ species was reported to be stable in solution; hence we assume the assembly of the hydrated $[Bi_6O_{4+x}(OH)_{4-x}]^{(6-x)+}$ ion into a polyacrylate matrix.[21,29] In addition to compound **1**, bismuth(III) nitrate pentahydrate and $[Bi_6O_4(OH)_4](NO_3)_6\cdot H_2O$ were tested as inorganic components for the synthesis of organic–inorganic hybrid materials. However, the reaction of these bismuth(III) nitrates with Sokalan® PA15 gave insoluble materials. The precipitate of the hybrid material obtained by the complexation of Sokalan® PA15 with $[Bi_6O_4(OH)_4(OTf)_6(CH_3CN)_6]\cdot 2CH_3CN$ (**1**) has a bismuth content of 8.7%. IR spectra and XPS data verify the complete exchange of triflate groups by carboxylate groups. TEM images of the hybrid material show bismuth-containing agglomerates with diameters between 1 and 15 nm, smaller agglomerates showing up more frequently (Figure 6). Figure 7 shows a selected area with particles in the range from 1.0 to 2.5 nm in diameter. The larger agglomerates most likely arise from the clustering of $[Bi_6O_{4+x}(OH)_{4-x}]^{(6-x)+}$–polyacrylate complexes, which might result from aggregation upon preparation of the TEM grids. In order to get a better idea of the particle-size distribution within the hybrid material, dynamic light scattering (DLS) measurements of Sokalan® PA15 and the hybrid material were performed in aqueous solution. For Sokalan® PA15 and the hybrid material, hydrodynamic mean diameters of 2.6 nm and 3.2 nm, respectively, were measured. We suggest the existence of a mixture of polyacrylate chains and complexes consisting of polyacrylate and $[Bi_6O_{4+x}(OH)_{4-x}]^{(6-x)+}$ from the hybrid material.

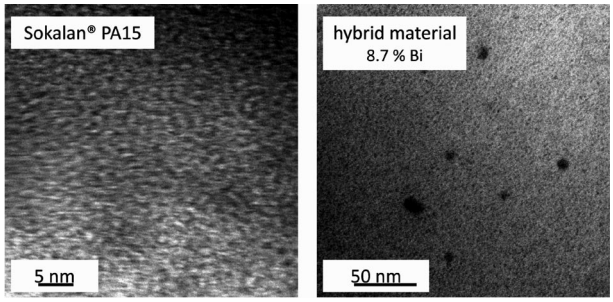

Figure 6. TEM images of Sokalan® PA15 (pure polymer, left) and the resulting hybrid material (right). Chemical analysis of the hybrid material gave a bismuth content of 8.7%. The dark areas were identified as bismuth-containing particles by electron energy loss spectroscopy (EELS).

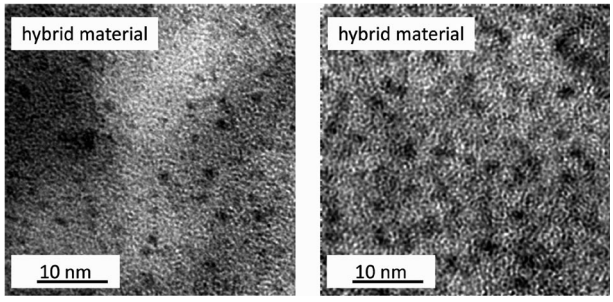

Figure 7. TEM images of the hybrid material showing different areas of the sample. The diameters of the bismuth-containing particles range from 1.0 to 2.5 nm.

Because it was not possible to distinguish the two species by DLS (most probably as a result of dynamic exchange reactions), we decided to perform molecular dynamics simulations. Among the complexes of polyacrylate and $[Bi_6O_{4+x}(OH)_{4-x}]^{(6-x)+}$ clusters, it is reasonable to expect $x = 0$, that is $[Bi_6O_4(OH)_4]^{6+}$, to represent the least stable configuration. As a lower estimate, we elucidated the interplay of $[Bi_6O_4(OH)_4]^{6+}$ ions and the Sokalan solution, a series of molecular dynamics simulations were performed on the basis of empirical interaction potentials.[30] By employing the Kawska–Zahn approach to model crystal aggregation, the association of polyacrylate (Sokalan® PA15) and sodium ions to $[Bi_6O_4(OH)_4]^{6+}$ was studied in aqueous solution.[31] The association of a single polyacrylate ion may already imply considerable structural changes in the $[Bi_6O_4(OH)_4]^{6+}$ ion. In two out of three simulation runs (taken as a rough estimate from ten independent runs), the cluster was degenerated from an octahedral motif to a tetrahedral motif (Figure 8). After this association step, the structural motifs remain unchanged in the course of Na^+ ion association or the aggregation of a further polyacrylate ion. For each simulation run, the polyacrylate chains were observed to enwrap the $[Bi_6O_4(OH)_4]^{6+}$ cluster by forming electrostatic bonds, which prevent Bi^{3+}, O^{2-}, and OH^- dissociation to the solvent within relaxation runs of 5 ns. Moreover, agglomerates of $[Bi_6O_4(OH)_4]^{6+}$ and two polyacrylate ions were found to form compact structures, which effectively shielded the bismuth oxido cluster from the association of further polyacrylate ions (Figure 8). Hence, a particularly stable complex consisting of $[Bi_6O_4(OH)_4]^{6+}$, two polyacrylate molecules, and sodium ions is obtained. The sodium ions tend to partially dissolve into the aqueous solution, causing an effective aggregate charge of –4 to –7. Similarly, the degenerated bismuth oxido cluster reacts with a second polyacrylate ion to give a stable aggregate. The diameters of both aggregates were found to be 2–3 nm, which is in accordance with experimental values.

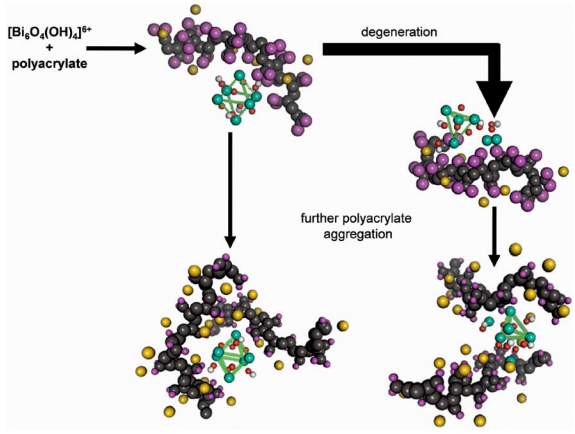

Figure 8. Molecular dynamics snapshots demonstrating the complexation behavior of bismuth oxido cluster **1** (Bi: cyan, O: red, H: white), polyacrylate (C: gray, O: magenta) and sodium ions (yellow) in aqueous solution (not shown). In two thirds of the simulation runs, the complexation of $[Bi_6O_4(OH)_4]^{6+}$ with one polyacrylate chain causes the degeneration of the hexanuclear bismuth oxido unit to a tetrahedral species. Both species react with a second polyacrylate.

Studies on the thermal behavior of the hybrid material and the polymer Sokalan® PA15 were carried out. TG thermograms of both compounds show two decomposition steps. In the first step, water is released between 30 and 243 °C. An adsorbed water content of 24.5% was determined for the hybrid material. Nearly the same water content (24.7%) was found for the pure polyacrylate. From 243 °C to 500 °C, the decomposition of the polyacrylate matrix into carbon dioxide and hydrocarbons takes place. The decomposition of the pure polyacrylate Sokalan® PA15 gave a mass loss of 51.2%. For the hybrid material, a weight loss of 49.7% was observed. The difference of 1.5% is in agreement with the bismuth content of the hybrid material. The complexation of the bismuth oxido species causes the melting point of the polyacrylate matrix to decrease, as shown by DSC measurements. While the pure sodium polyacrylate melts at 173 °C, the hybrid material has a melting point at 128 °C. At 480 °C, another endothermic peak associated with a weight loss was observed. We propose the in situ formation of bismuth oxido carbonate during the decomposition of the hybrid material and its subsequent degradation to bismuth oxide. The X-ray powder diffraction of the decomposition residue of the hybrid material is indicative of the formation of β-Bi_2O_3 (JCPDS No. 027–0050), which is in accordance with previous reports on the thermal decomposition of $(BiO)_2CO_3$ to give β-Bi_2O_3.[32]

Conclusions

Starting from $[Bi_6O_4(OH)_4](NO_3)_6{\cdot}H_2O$, it is possible to synthesize the hexanuclear bismuth oxido cluster $[Bi_6O_4(OH)_4(OTf)_6(CH_3CN)_6]{\cdot}2CH_3CN$ (**1**), which is highly soluble in water and polar organic solvents. Thus, the cluster is suitable for the synthesis of organic–inorganic hybrid materials from homogeneous solution. We have shown herein the synthesis of a water soluble hybrid material starting from sodium polyacrylate and compound **1**. TEM images of the resulting hybrid material show a narrow size distribution of the polyacrylate-modified bismuth oxido particles. By means of molecular dynamics simulation, we could demonstrate the complexation behavior between the $[Bi_6O_{4+x}(OH)_{4-x}]^{(6-x)+}$ cation and polyacrylate in aqueous solution. Partial degradation of the hexanuclear bismuth oxido species does occur, which is predicted by the molecular dynamics simulation. Sokalan® PA15 effectively prevents further aggregation of the bismuth oxido clusters. Thus, control of the cluster size and solubility by addition of additives such as polyacrylate seems to be possible, which might give rise to novel radiopaque organic–inorganic hybrid materials.

Experimental Section

General Remarks

Toluene was distilled from sodium prior to use. $Bi(NO_3)_3{\cdot}5H_2O$ (Riedel-de Haën), CF_3SO_3H, $Me_3SiO_3SCF_3$ (Alfa Aesar), and Sokalan® PA15 (BASF) were used as received. The bismuth content was quantitatively determined by complexometric titration of EDTA with xylenol orange.[33] The elemental analysis of **1** was performed with a LECO-CHNS-932 analyzer. The elemental analyses of the hybrid materials were carried out with a FlashAE 112 Thermo-CHN analyzer.

$[Bi_6O_4(OH)_4](NO_3)_6{\cdot}H_2O$, $[Bi_6O_4(OH)_4(OTf)_6(CH_3CN)_6]{\cdot}2CH_3CN$ (**1**) and the decomposition residue of the hybrid material were analyzed by X-ray powder diffraction at 25 °C with a STOE-StadiP diffractometer having monochromated Cu-K_α radiation. The X-ray structure determination for compound **1** was performed by using an Oxford Gemini S diffractometer with graphite-monochromated Mo-K_α radiation at 100 K (see Table 1). The structure was solved by direct methods with SHELXS-97 and refined with SHELXL-97. All non-hydrogen atoms were refined with anisotropic thermal parameters. The hydrogen atoms of the bismuth oxido core were placed in observed positions. The residual ones were placed in geometrically calculated positions. Disordered atoms were found with occupancies of 0.555 [C(4), F(10)–F(11)] and 0.445 [C(4)′, F(10)′–F(12)′] and were refined at two positions. The figures were created by DIAMOND (release 3.0, 2005).

Transmission electron microscopy (TEM) images were obtained with a 200 kV Phillips CM20 FEG transmission electron microscope. For sample preparation, a copper grid (Ø = 3.0 mm) was coated with a thin film of the hybrid material: Acetonitrile was added to an aqueous solution of the hybrid material to bring about a phase separation. Then, the copper grid was dipped into the deposited liquid polymer phase to generate a thin film. Before use, the sample was dried in vacuo. The particle-size distribution was determined by dynamic light scattering (DLS) with a Viscotek DLS 802 instrument. The measurements of aqueous solutions of the hybrid material and Sokalan® PA15 were carried out by using a quartz glass cell.

Thermogravimetric measurements were performed with a Perkin–Elmer TGA 7 instrument at a heating rate of 5 °C/min to a maximum temperature of 700 °C in flowing helium with platinum as reference material. The DSC thermograms were made by using a Pyris-I-DSC instrument from Perkin–Elmer. The measurements were performed in a capped platinum pan to a maximum temperature of 500 °C with nitrogen as purging gas. The residues of the thermogravimetric analysis were examined by X-ray powder diffraction. ^1H and ^{13}C NMR spectra were recorded with an Avance 250 Bruker NMR spectrometer at 250.13 and 62.90 MHz, respectively. Chemical shifts, δ, are given in ppm and are referenced against $(CH_3)_4Si$. ATR-FTIR spectra were recorded with a BioRad FTS-165 spectrometer by using a golden gate sample adapter.

$[Bi_6O_4(OH)_4](NO_3)_6{\cdot}H_2O$: The synthesis was carried out according to ref.[24] The compound was dried at 80 °C (3×10^{-3} mbar) for 12 h. The X-ray powder pattern is in agreement with that of $[Bi_6O_4(OH)_4](NO_3)_6{\cdot}H_2O$ (JCPDS No. 71–1360).[20] M.p. >300 °C (decomp.). IR: $\tilde{\nu}$ = 3524 (w), 3202 (w), 1286 (s), 1040 (m), 809 (m), 722 (m), 547 cm^{-1} (s).

$[Bi_6O_4(OH)_4(OTf)_6(CH_3CN)_6]{\cdot}2CH_3CN$ (1)

Synthesis by Method a: CF_3SO_3H was added dropwise to a suspension of $[Bi_6O_4(OH)_4](NO_3)_6{\cdot}H_2O$ (5.0 g, 2.8 mmol) in toluene (60 mL, 3.5 g, 23.2 mmol). After stirring at 60 °C for 16 h, the brown solid formed was filtered off, washed with toluene, and dried at 40 °C (3×10^{-3} mbar). Colorless crystals suitable for single-crystal X-ray diffraction were obtained from acetonitrile/chloroform (3.5 g, 55%).

Synthesis by Method b: $Me_3SiO_3SCF_3$ was added dropwise to a suspension of $[Bi_6O_4(OH)_4](NO_3)_6{\cdot}H_2O$ (5.0 g, 2.8 mmol) in toluene (60 mL, 7.4 g, 33.4 mmol). Stirring at 60 °C for 16 h gave a dark brown solid. The precipitate was filtered off, washed with toluene, and dried at 40 °C (3×10^{-3} mbar). Colorless crystals were obtained from acetonitrile/chloroform.

Analytical Data: The XRPD corresponds to $[Bi_6O_4(OH)_4(OTf)_6(CH_3CN)_6]{\cdot}2CH_3CN$ (**1**). M.p. >300 °C (decomp.). ^1H NMR (250.1 MHz, CD_3CN) for **1** (0.036 mol/L): δ = 1.97 (s, CH_3), 3.04 (br. s, OH) ppm; for **1** (0.052 mol/L): δ = 1.97 (s, CH_3), 3.36 (br. s, OH) ppm; for **1** (0.070 mol/L): δ = 1.97 (s, CH_3), 3.57 (br. s, OH) ppm; for **1** (0.088 mol/L): δ = 1.97 (s, CH_3), 3.75 (br. s, OH) ppm. $^{13}C\{^1H\}$ NMR (62.9 MHz, [D$_6$]DMSO): δ = 121.1 (q, ^1J = 322.0 Hz, CF_3) ppm. IR: $\tilde{\nu}$ = 3467 (m), 1213 (s), 1016 (s), 622 (s), 568 (s), 510 cm^{-1} (s). $C_6H_4Bi_6F_{18}O_{26}S_6$ (2280.31): calcd. C 3.2, H 0.2; found C 3.5, H 0.1.

Crystal Data: $C_{22}H_{28}Bi_6F_{18}N_8O_{26}S_6$, M = 2608.76, crystal size $0.6\times0.05\times0.05$ mm, monoclinic, space group $P2_1/n$, Z = 4, a = 12.6443(8) Å, b = 18.1326(4) Å, c = 27.0115(9) Å, β = 96.787(4)°, V = 6149.6(5) Å^3, D_c = 2.947 g/cm^3, F(000) = 4952, μ(Mo-K_α) = 0.71073 Å, T = 100 K, $2.92 \le 2\theta \le 26.09$, completeness to 2θ: 98.4%, max./min. residual electron density: 3.183/–3.469 e/Å^3. Of a total of 55116 reflections collected, 12031 reflections were independent (R_{int} = 0.0585). Final $R1$ = 0.0565 [for 12031 reflections $I>2\sigma(I)$] and $wR2$ = 0.1084 (all data).

CCDC-781174 contains the supplementary crystallographic data for this paper. These data can be obtained free of charge from The Cambridge Crystallographic Data Centre via www.ccdc.cam.ac.uk/data_request/cif.

Preparation of the Hybrid Material: An aqueous solution of **1** (20 mL, 0.2 g, 0.1 mmol) and an aqueous solution of Sokalan®

PA15 (50 mL, 2.2 g) were mixed and stirred for 1 h at room temperature. The reaction solution was added in portions to acetone at 0 °C. After centrifugation and washing twice with acetone, a gel was obtained that was dried in vacuo to give a transparent solid material (0.4 g). 100 mg of the hybrid material contains 8.7 mg of bismuth. $^{13}C\{^1H\}$ CP MAS NMR (100.6 MHz): δ = 32.8, 40.7, 46.8 (CH_2), 67.2 (CH), 185.7 (CO) ppm. IR: $\tilde{\nu}$ = 3270 (m), 2921 (m), 2852 (w), 1555 (s), 1457 (m), 1397 (s), 1323 (m), 1049 (m), 850 (m), 783 (m), 618 (m), 508 cm^{-1} (s); chemical analysis (%): found C 27.9, H 4.4, Na 15.5, Bi 8.7.

Molecular Dynamics Simulations: The starting point was chosen as the $[Bi_6O_4(OH)_4]^{6+}$ cluster, whose initial structure was adopted from experimental data. By using a docking/relaxation procedure, which is described in detail in ref.,[31] the association of up to three polyacrylate ions and a sufficiently large number of Na^+ ions to allow charge neutrality was investigated in aqueous solution. In the overall system, the solutes are embedded in more than 4000 water molecules, placed in a periodic simulation cell of approximate dimensions of 5 nm × 5 nm × 5 nm. Empirical force fields were taken from ref.[30] The molecular dynamics runs were performed at ambient conditions, applying constant pressure (1 atm) and constant temperature (300 K). With a time-step of 1 fs, relaxation runs of 5 ns were performed after each association step. While structural relaxation was observed to be much faster (on the ps scale), long-termed relaxation allowed the reliable assessment of Na^+ dissociation and hence determination of the effective charge of the complex as described in the Results and Discussion.

Acknowledgments

We acknowledge the Deutsche Forschungsgemeinschaft (SPP1415) for financial support and the BASF for providing Sokalan®-based polymers.

[1] J. R. Lambert, P. Midolo, *Aliment. Pharm. Therap.* **1997**, *11*, 27–33.
[2] H. Ippen, *Hautarzt* **1997**, *48*, 424.
[3] a) S. Serefis, *Arch. Dermatol. Syph.* **1934**, *171*, 1–98; b) A. Larsen, M. Stoltenberg, M. J. West, G. Danscher, *J. Appl. Toxicol.* **2005**, *25*, 383–392; c) J. Boertz, L. M. Hartmann, M. Sulkowski, J. Hippler, F. Mosel, R. A. Diaz-Bone, K. Michalke, A. W. Rettenmaier, A. V. Hirner, *Drug Metab. Dispos.* **2009**, *37*, 352–358; d) M. Hollmann, J. Boertz, E. Dopp, J. Hippler, A. V. Hirner, *Metallomics* **2010**, *2*, 52–56.
[4] N. Burford, G. G. Briand, *Chem. Rev.* **1999**, *99*, 2601–2657.
[5] a) G. F. Nordberg, *Handbook on the Toxicology of Metals*, 3 ed., Elsevier, **2007**; b) Y. M. Yukhin, T. V. Daminova, L. I. Afonina, B. B. Bokhonov, O. A. Logutenko, A. I. Aparnev, K. Y. Mikhailov, T. A. Udalova, V. I. Evseenko, *Chem. Sustain. Develop.* **2004**, *12*, 395–401.
[6] H. Sun, H. Li, I. Harvey, P. J. Sadler, *J. Biol. Chem.* **1999**, *274*, 29094–29101.
[7] O. Rabin, J. M. Perez, J. Grimm, G. Wojtkiewicz, R. Weissleder, *Nat. Mater.* **2006**, *5*, 118–122.
[8] S. Abdulghani, S. N. Nazhat, J. C. Behiri, S. Deb, *J. Biomater. Sci. Polym. Ed.* **2003**, *14*, 1229–1242.
[9] J. A. Wimhurst, R. A. Brooks, N. Rushton, *J. Bone Joint Surg. Br.* **2001**, *83B*, 588–592.
[10] a) F. Mottu, D. A. Rufenacht, E. Doelker, *Invest. Radiol.* **1999**, *34*, 323–335; b) K. Saito, F. Oosato, Y. Ochiai, T. Tanaka, M. Tetsuka, I. Inage, JP 1993–31467, Mitsui Toatsu Chemicals, Lion Corp, Japan, **1994**; c) V. P. Chuev, M. G. Priemskaya, Y. V. Barkhatov, E. A. Kuz'ima, RU 2001–103631, Zakrytoe Aktsionernoe Obshchestvo "Vladmiva", Russia, **2002**; d) M. Kondo, JP 1993–184418, Japan, **1995**; e) L. A. Ivanova, V. S. Ivanov, O. F. Konobevtsev, V. N. Kondaurov, A. A. Yakovenko, E. V. Ivanova, SU 1986–4153955, Central Scientific-Research Institute of Stomatology, Central Institute for Advanced Training of Physicians USSR, I. M. Sechenov State Medical Institute, USSR, **1991**; f) E. A. Bortoluzzi, J. M. Guerreiro-Tanomaru, M. A. Duarte, *Oral Surg. Oral Med. Oral Pathol.* **2009**, *108*, 628–632.
[11] Y. Delaviz, Z. X. Zhang, I. Cabasso, J. Smid, *J. Appl. Polym. Sci.* **1990**, *40*, 835–843.
[12] D. Mansfeld, M. Mehring, M. Schürmann, *Angew. Chem. Int. Ed.* **2005**, *44*, 245–249.
[13] M. Mehring, D. Mansfeld, S. Paalasmaa, M. Schürmann, *Chem. Eur. J.* **2006**, *12*, 1767–1781.
[14] a) P. C. Andrews, G. B. Deacon, C. M. Forsyth, P. C. Junk, I. Kumar, M. Maguire, *Angew. Chem. Int. Ed.* **2006**, *45*, 5638–5642; b) E. Dikarev, H. Zhang, B. Li, *Angew. Chem. Int. Ed.* **2006**, *45*, 5448–5451.
[15] D. L. Rogow, H. Fei, D. P. Brennan, M. Ikehata, P. Y. Zavalij, A. G. Oliver, S. R. J. Oliver, *Inorg. Chem.* **2010**, *49*, 5619–5624.
[16] M. Mehring, M. Schürmann, *Chem. Commun.* **2001**, 2354–2355.
[17] X. Kou, X. Wang, D. Mendoza-Espinosa, L. N. Zakharov, A. L. Rheingold, W. H. Watson, K. A. Brien, L. K. Jayarathna, T. A. Hanna, *Inorg. Chem.* **2009**, *48*, 11002–11016.
[18] J. P. Sachetto, US 1999–308161, Medeva Europe Ltd., United States, **1999**.
[19] B. Sundvall, *Acta Chem. Scand.* **1979**, *A33*, 219–224.
[20] F. Lazarini, *Acta Crystallogr., Sect. B* **1979**, *35*, 448–450.
[21] J. Näslund, I. Persson, M. Sandström, *Inorg. Chem.* **2000**, *39*, 4012–4021.
[22] B. Sundvall, *Inorg. Chem.* **1983**, *22*, 1906–1912.
[23] a) B. Kugel, W. Frank, *Z. Anorg. Allg. Chem.* **2002**, *628*, 2178; b) M. Kawamura, D. Cui, S. Shimada, *Tetrahedron* **2006**, *62*, 9201–9209.
[24] A. N. Christensen, M. A. Chevallier, J. Skibsted, B. B. Iversen, *J. Chem. Soc., Dalton Trans.* **2000**, 265–270.
[25] N. Henry, O. Mentre, F. Abraham, E. J. MacLean, P. Roussel, *J. Solid State Chem.* **2006**, *179*, 3087–3094.
[26] a) N. C. Norman, *Chemistry of Arsenic, Antimony and Bismuth*, 1st ed., Blackie Academic and Professional, London, **1998**; b) M. Mehring, *Coord. Chem. Rev.* **2007**, *251*, 974–1006.
[27] a) M. Mehring, D. Mansfeld, M. Schürmann, *Z. Anorg. Allg. Chem.* **2004**, *630*, 452–461; b) D. Mansfeld, M. Mehring, *Z. Anorg. Allg. Chem.* **2005**, *631*, 2429–2432.
[28] http://worldaccount.basf.com/wa/NAFTA~en_US/Catalog/ChemicalsNAFTA/pi/BASF/Brand/sokalan.
[29] a) A. F. Hollemann, E. Wiberg, *Lehrbuch der Anorganischen Chemie*, 102nd ed., Walter de Gruyter, Berlin, **2007**; b) K.-H. Tytko, *Chem. Unserer Zeit* **1979**, *13*, 184–194.
[30] a) J. Wang, R. M. Wolf, J. W. Caldwell, P. A. Kollman, D. A. Case, *J. Comput. Chem.* **2004**, *25*, 1157–1174; b) C. I. Bayly, P. Cieplak, W. Cornell, P. A. Kollman, *J. Phys. Chem.* **1993**, *97*, 10269–10280.
[31] a) A. Kawska, J. Brickmann, R. Kniep, O. Hochrein, D. Zahn, *J. Chem. Phys.* **2006**, *124*, 24513; b) A. Kawska, O. Hochrein, J. Brickmann, R. Kniep, D. Zahn, *Angew. Chem. Int. Ed.* **2008**, *47*, 4982–4985; c) T. Milek, P. Duchstein, G. Seifert, D. Zahn, *ChemPhysChem* **2010**, *11*, 847–852.
[32] S. K. Blower, C. Greaves, *Acta Crystallogr., Sect. C* **1988**, *44*, 587–589.
[33] G. Jander, K. F. Jahr, G. Schulze, J. Simon, *Maßanalyse-Theorie und Praxis der Titrationen mit chemischen und physikalischen Indikationen*, 16th ed., Walter de Gruyter, Berlin, New York, **2003**.

Received: July 9, 2010
Published Online: September 20, 2010

